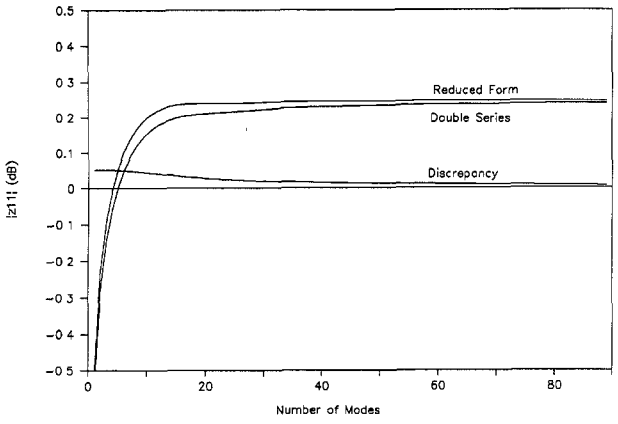

Fig. 2. Z_{11} for disk.

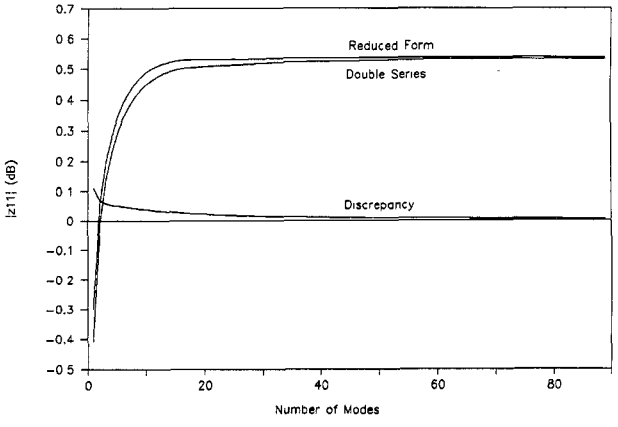

Fig. 3. Z_{11} for ring.

for the circular disk for both the double series and the reduced form and the discrepancy between them. Fig. 3 shows the values of Z_{11} for the annular ring for both the double series and the reduced form as well as the discrepancy between them.

VI. Conclusion

The Green's functions for the circular disk and the annular ring have been reduced to single-series forms in a mathematically direct manner, eliminating the need for the eigenvalues and, as a consequence, improving the speed and accuracy of the computation.

Acknowledgment

The authors wish to thank Dr. M. Page for providing experimental results to validate the theory.

References

[1] K. C. Gupta *et al.*, *Computer Aided Design of Microwave Circuits*. Norwood, MA: Artech House, 1981, p. 247.

[2] H. S. Carslaw, "The Green's function for the equation $\nabla^2 u + \kappa^2 u = 0$," *Proc. London Math. Soc.*, vol. 15, pp. 84–93. Apr. 1916.

[3] A. Benalla and K. C. Gupta, "Faster computation of Z-matrices for rectangular segments in planar microstrip circuits," *IEEE Trans. Microwave Theory Tech.*, vol. MTT-34, pp. 733–763, June 1986.

[4] M. D. Abouzahra and K. C. Gupta, "Multiple-port power divider/combiner circuits using circular microstrip disk configurations," *IEEE Trans. Microwave Theory Tech.*, vol. MTT-35, pp. 1296–1302, Dec. 1987.

[5] J. C. C. A. Kneser, "Die Entwicklung Beliebiger Funktionen von beschränkter Schwankung nach Besselschen," *Math. Ann.*, Bd. 63, pp. 510–517, 1907.

[6] G. N. Watson, *A Treatise on The Theory of Bessel Functions*. Cambridge, England: Cambridge University Press, 1966, p. 499.

A Surface Integral Equation Method for the Finite Element Solution of Waveguide Discontinuity Problems

Omar M. Ramahi and Raj Mittra

Abstract—**The surface integral equation method, which is typically employed in the finite element solution of open-region scattering problems, has been applied in this paper to the solution of waveguide discontinuity problems. The major advantage offered by the surface integral equation approach over other available methods is that it allows the mesh-truncating boundaries to be brought as close to the discontinuity as possible, thus helping to reduce the size of the system matrix. In addition, unlike the mode matching technique, the surface integral equation formulation does not require the solution of any auxiliary matrix system. Numerical results are presented to illustrate the validity of the formulation.**

I. Introduction

When designing waveguide devices, it is often necessary to introduce discontinuities or loads that are used for different purposes such as phase shifting or power matching to a specific load or termination. The analysis of such waveguide junctions or discontinuities has traditionally been carried out using the mode-matching techniques and the integral equation method [1], [2]. However, when the discontinuities are irregularly shaped or involve inhomogeneous or anisotropic objects, the integral equation methods become quite laborious and difficult to apply. For such complex and irregularly shaped geometries, either the finite element or the finite difference method becomes the preferred choice. Additionally, the finite methods generate highly sparse and banded matrices which can be efficiently handled using special algorithms.

When using the finite element (or the finite difference) method to solve boundary values problems such as waveguide discontinuities, two major consideration arise. First, it is always desirable to bring the mesh-truncating boundary as close as possible to the discontinuity junction in order to reduce the number of mesh points and, hence, the size of the associated matrix. Second, a boundary condition must be imposed on the terminal boundaries such that it accurately reflects the proper field behavior there. The task of devising an efficient solution procedure that accommodates the above two considerations is the principal subject of discussion in this paper.

Conventionally, finite element formulations of the waveguide discontinuity problem are based upon the truncation of the finite element mesh region at a distance where the amplitudes of the evanescent modes become negligible, and then the imposition of a Dirichlet or a Neumann boundary condition [3], [4]. Such construction offers the advantage of generating a sparse matrix system. In certain applications, such as the modeling of electromagnetic pulse simulators, the width of the simulator/waveguide may range from a fraction of a wavelength to tens of

Manuscript received June 5, 1990; revised October 15, 1990.

The authors are with the Department of Electrical and Computer Engineering, University of Illinois, Urbana, IL 61801.

IEEE Log Number 9042351.

wavelengths, which gives rise to evanescent modes having significant amplitudes within an appreciable distance from the discontinuity. Consequently, to guarantee sufficient accuracy of the finite element solution, it becomes necessary to extend the mesh region such that the amplitudes of the evanescent modes become negligible at the truncation boundary. Naturally, this renders the solution procedure very impractical. Another widely used procedure is to use the finite element method in conjunction with the mode-matching technique. Although this method allows the outer boundary to be brought close to the discontinuity, and thus minimizes the size of the system matrix, it suffers from two disadvantages: (i) it requires the solution of an additional auxiliary matrix system and (ii) it has the potential of generating spurious modes.

In this paper, we use the surface integral equation as a boundary condition for the finite element mesh region. The use of the surface integral equation as a boundary condition for electromagnetic problems was first reported in the work of McDonald and Wexler [5], where it was applied to solve the Poisson equation. Others have used the method to solve open-region electromagnetic radiation problems [6], [7]. In [8] and [9], the boundary element method, which in its theoretical development parallels the surface integral approach, has been employed to treat waveguide discontinuity problems. The disadvantage in using the boundary element method, however, arises when dealing with multimedia problems [8].

Because the surface integral equation is an exact boundary condition, it can handle both the propagating and evanescent modes at the truncation boundary. This, in turn, allows us to bring the outer boundaries very close to the discontinuity. While this feature is also realized by the mode matching technique, the surface integral equation approach has the advantage that it does not introduce any spurious modes into the solution. In addition, the surface integral equation method requires the solution of the system matrix only once; thus, the need to solve an auxiliary matrix system is obviated. The complete procedure for the formulation of the surface integral equation appears in Section II. In Section III, we present numerical results for a simple iris discontinuity problem, where a comparison is made with the results obtained by using the method of moments. Results are also presented for a waveguide containing dielectric obstacles, and a comparison is made with the exact solution wherever possible. Section IV presents some concluding remarks.

II. Surface Integral Equation in the Finite Element Solution

In this section, we present the formulation of the surface integral equation method and specialize it to the waveguide discontinuity problem. Only the parallel-plate waveguide will be considered in this work, However, the theoretical formulation presented in this paper can be extended to rectangular or cylindrical waveguides as well.

Consider Fig. 1, which shows a multiport parallel-plate waveguide device with an irregularly shaped junction containing inhomogeneous source-free material. It will be assumed, without loss of generality, that the source field is incident from the port labeled the excitation port (see Fig. 1). The finite element mesh region will then include the discontinuity and will be bound by the layers Γ_{Bi}, $i = 0,2,\cdots,N$. Let Ω^{int} denote the finite element region. We use the conventional finite element formulation [10], [11], in conjunction with Green's theorem, to obtain the weak form of the Helmholz equation

$$\int_{\Omega} \frac{1}{\epsilon(x)} \nabla H \cdot \nabla v - k^2 \mu(x) H v \, ds = \int_{\partial\Omega} \frac{1}{\epsilon(x)} v \frac{\partial H}{\partial n} dl \quad (1)$$

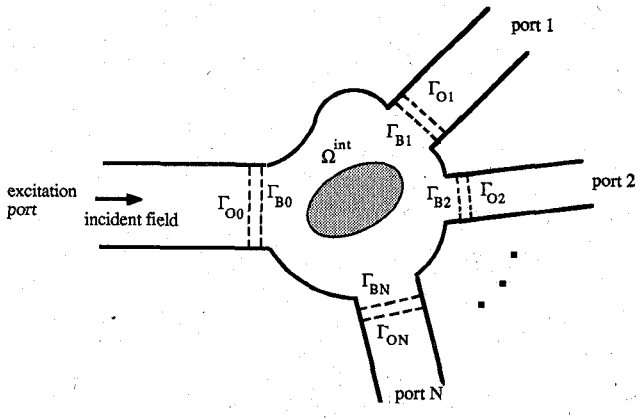

Fig. 1. Geometry for a multiport waveguide system.

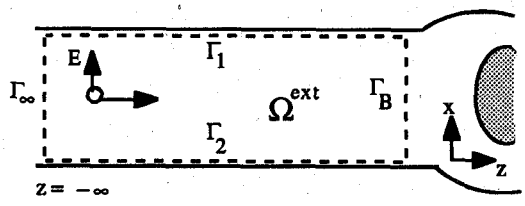

Fig. 2. Geometry for the construction of the surface integral equation.

where H is the y component of the unknown total magnetic field, and v is the testing function.

Next, we divide the solution region Ω^{int} into triangular elements and approximate the unknown field H over each of the elements by a set of interpolating functions:

$$H(x) = \sum_{i=1}^{3} H_i \psi_i(x). \quad (2)$$

For the first-order linear triangular elements, the ψ_i's are linear interpolatory functions with a finite support covering a single triangular element, and the H_i's are the nodal field values at the vertices of each element. By choosing the testing functions identical to those for the ψ_i's, and after substituting (2) into (1), we arrive at the typical finite element matrix system

$$\boldsymbol{MU} = \boldsymbol{B}$$

which is symbolically represented as

$$\begin{bmatrix} \boldsymbol{M}_{OO} & \boldsymbol{M}_{OB} & \boldsymbol{0} \\ \boldsymbol{M}_{BO} & \boldsymbol{M}_{BB} & \boldsymbol{M}_{BC} \\ \boldsymbol{0} & \boldsymbol{M}_{CB} & \boldsymbol{M}_{CC} \end{bmatrix} \begin{bmatrix} \boldsymbol{U}_O \\ \boldsymbol{U}_B \\ \boldsymbol{U}_C \end{bmatrix} = \begin{bmatrix} \boldsymbol{B}_O \\ \boldsymbol{B}_B \\ \boldsymbol{B}_C \end{bmatrix} \quad (3)$$

where $\boldsymbol{M}$ is the stiffness matrix, and $\boldsymbol{U}_O$, $\boldsymbol{U}_B$, and $\boldsymbol{U}_C$ are column vectors corresponding to the nodal field values at the layers $\Gamma_{O0},\Gamma_{O1},\cdots,\Gamma_{ON}$, the layers $\Gamma_{B0},\Gamma_{B1},\cdots,\Gamma_{BN}$, and the interior region of the discontinuity Ω^{int}, respectively (see Fig. 1). The Γ_B boundary layer defines the boundary of the finite element mesh. The outermost boundary layer, Γ_O, is constructed for the enforcement of the boundary conditions, as will be discussed below.

Returning to (3), we note that our boundary value problem cannot be fully specified unless the matrix $\boldsymbol{B}$, particularly $\boldsymbol{B}_O$, is explicitly known. This, in turn, requires enforcing a boundary condition at each of the Γ_B layers.

The surface integral equation is constructed by expressing the field in the interior of each of the waveguides in terms of the field and its normal derivative on the respective waveguide walls and its terminal boundaries (see Fig. 2). Invoking the Green's

function theorem [12], we have

$$H(x)=\int_{\partial\Omega^{ext}} G(x/x')\nabla H(x')\cdot\hat{n}_B - H(x')\nabla G(x/x')\cdot\hat{n}_B\, d\zeta' \tag{4}$$

where x' is the integration coordinate, n_B is the outward normal unit vector from $\partial\Omega^{ext}$, and G is the Green's function.

The surface integral equation in (4) can be simplified by using a Green's function of the first kind, $G^{(1)}$, which is defined as the solution of

$$\nabla^2 G^{(1)}(x/x')+k^2 G^{(1)}(x/x')=-\delta(x-x')$$

Subject to the boundary condition

$$G^{(1)}=0 \qquad \text{on } \partial\Omega^{ext}.$$

The Green's function of the first kind can, therefore, be obtained as the solution of the parallel-plate waveguide when terminated at the layer Γ_B with a perfect magnetic wall. Since $G^{(1)}$ and H satisfy the radiation condition at $z=\pm\infty$, and $\partial H/\partial n=0$ on the waveguide walls Γ_1 and Γ_2, the surface integral equation reduces to

$$H(x)=u^{inc(1)}(x)+\int_{\partial\Omega^{ext}} gH(x')\nabla G(x/x')\cdot\hat{n}_B\, d\zeta' \tag{5}$$

where $u^{inc(1)}$ is defined as the total field in the presence of a perfect magnetic conductor placed at Γ_B.

An analytical expression for $\partial G^{(1)}/\partial n$ can be easily obtained, and is given by

$$\frac{\partial G^{(1)}}{\partial z'}(x/x')=\sum_{n=0}^{\infty}\frac{\epsilon_n}{a\Gamma_n}\cos\left(\frac{n\pi x}{a}\right)\cos\left(\frac{n\pi x'}{a}\right)e^{\Gamma_n(z-|z'|)}$$

where a is the width of the waveguide, $\Gamma_n=\sqrt{\{k_0^2-(n\pi/a)^2\}}$, and $\epsilon_n=1$ for $n=0$, and 2, otherwise. The use of Green's function of the first kind, $G^{(1)}$, also eliminates the need for the numerical differentiation that would otherwise be required to express the normal derivative of the field on the Γ_B boundary. This, in turn, leads to higher solution accuracy.

The use of the surface integral equation as a boundary condition for the finite element region (region of the discontinuity) requires transforming or descretizing (5) into a matrix equation that would eventually augment the finite element matrix system. This discretization can be accomplished in different ways depending on the interpolatory functions chosen to expand the field on the contours Γ_B. However, to maintain a consistent order of the approximation throughout the solution region vis-à-vis the finite element solution, and, furthermore, to ensure the proper preconditioning of the matrix system such that the sparsity of the matrix is maximized, we employ piecewise-linear basis functions. For simplicity, we choose basis functions that are identical to the basis functions used in the finite element region. Thus, expanding the scattered field over the contours Γ_B, in terms of linear basis functions, we have

$$H(\zeta)=\sum_{j=1}^{M}\sum_{i=1}^{2} H_i\psi_i(\zeta) \tag{6}$$

where $\psi_i(\zeta)$ is defined locally over the edge of each boundary element as

$$\psi_i(\zeta)=\begin{cases}1-\dfrac{\zeta}{h}, & i=1\\[2ex] \dfrac{\zeta}{h}, & i=2\end{cases}.$$

The first summation in (6) is taken over all elements, numbering M, that are tangential to the contours Γ_B, and the H_i's are the nodal field values at the layers Γ_B. Substituting (6) into (5), we arrive at the discretized version of the surface integral equation, viz.,

$$H(x_O)=-\sum_{j=1}^{M}\sum_{i=1}^{2} H_i\int_{\partial\Omega^{ext}}\psi(x_B)\nabla G^{(1)}(x_O/x_B)\cdot\hat{n}_B\, d\zeta'. \tag{7}$$

Finally, enforcing (7) at each of the Γ_O layer nodes gives the boundary matrix equation

$$U_O=SU_B+T \tag{8}$$

where S is an $M\times M$ matrix with elements defined as

$$s_{jk}=\int_{\partial e^{(j)}}\psi_2\nabla G^{(1)}(x_j/x_k)\cdot\hat{n}_B\, d\zeta' + \int_{\partial e^{(j)}}\psi_1\nabla G^{(1)}(x_j/x_k)\cdot\hat{n}_B\, d\zeta'$$

and $\partial e^{(j)}$ is the edge of element j. The column matrix T in (8) has the contribution from the excitation field which was assumed to be incident only from the excitation port.

The net result of the above construction is the transformation of the surface integral equation into an algebraic equation. Therefore, the matrix equation (8) can be interpreted as an algebraic boundary operator, or a matrix boundary condition for the system in (3). The final matrix system is arrived at by adding (8) to (3). This circumvents the need to evaluate the column

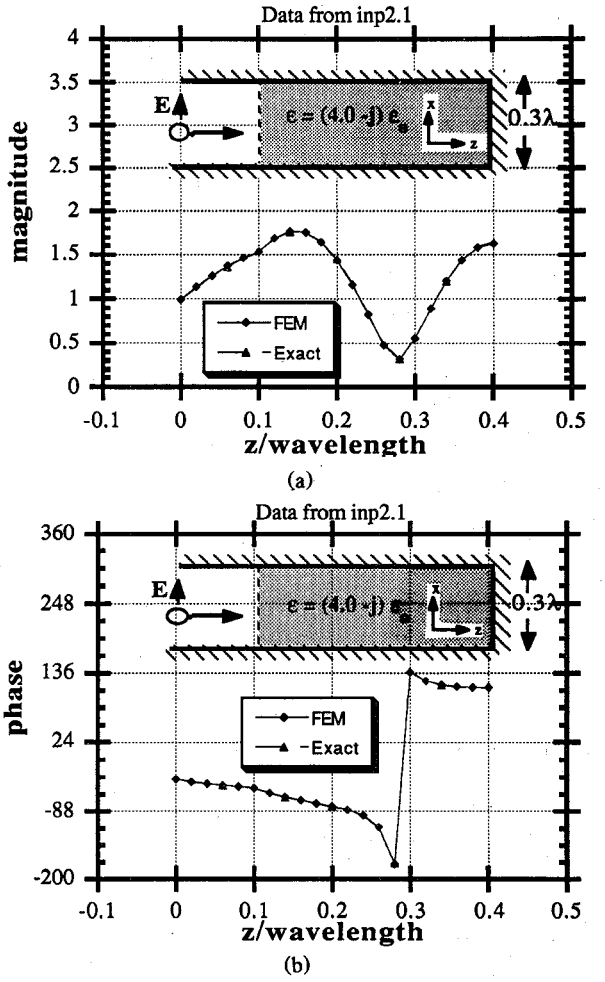

Fig. 3. Finite element (FEM) and exact solutions for the normalized total H-field distribution for a waveguide with a lossy uniform dielectric termination. Outer boundary Γ_B at $z=0$. (a) Magnitude. (b) Phase.

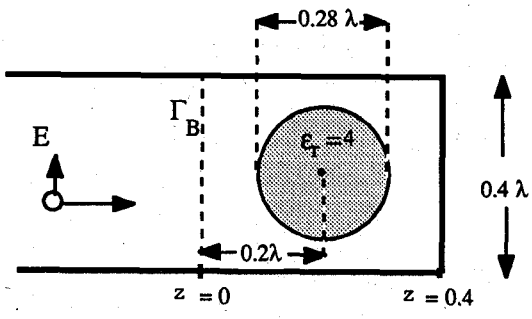

Fig. 4. Geometry for the parallel-plate waveguide with a dielectric circular cylinder. Outer boundary at Γ_B at $z = 0$.

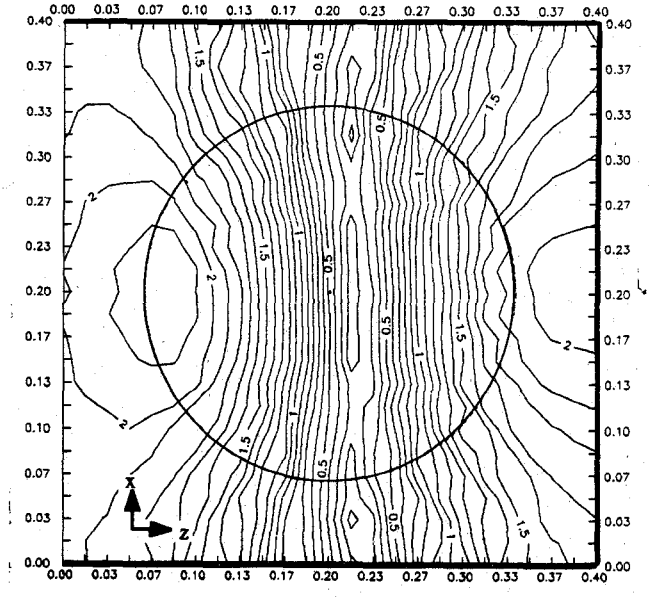

Fig. 5. Contour H-field plot for the cylinder loaded waveguide.

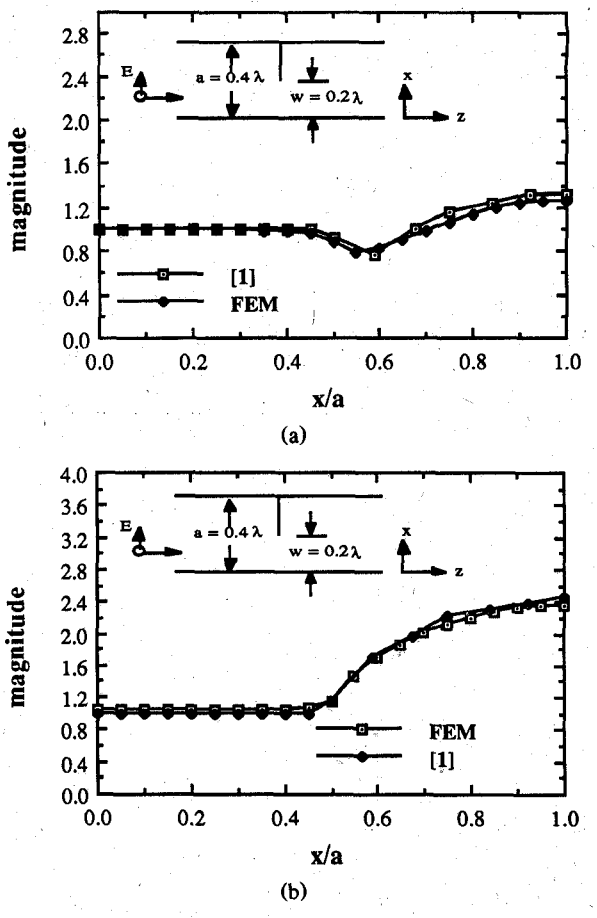

Fig. 6. Finite element (FEM) and Wiener–Hopf [1] solutions for the normalized magnitude of the aperture field distribution in an iris loaded (at $z = 0$) parallel-plate waveguide due to an incident TEM mode. Outer boundary Γ_B at $z = -0.2\lambda$, $+0.2\lambda$. (a) At the plane $z = 0^+$. (b) At the plane $z = 0^-$.

vector B_O by dispensing with the first row of the matrix M in (3) altogether. The resulting matrix reads

$$\begin{bmatrix} (M_{BO}S + M_{BB}) & M_{BC} \\ M_{CB} & M_{CC} \end{bmatrix} \begin{bmatrix} U_B \\ U_C \end{bmatrix} = \begin{bmatrix} B_B - B_{BO}T \\ B_C \end{bmatrix}. \quad (9)$$

A close observation of the matrix equation in (9) shows that the matrix blocks M_{CC} and M_{CB} are a direct result of the finite element descretization of the discontinuity region Ω^{int}; therefore, the largest block of the system matrix will be sparse. Only the row matrix corresponding to the boundary layer nodes U_B will result in a partially populated block.

III. Numerical Results

Based on the mathematical formulation outlined above, a finite element code was developed which incorporated the surface integral equation formulation. Three different simple geometries were studied in this work, and a comparison was made, whenever possible, with the results derived by using the analytical methods or the integral equation technique. While the formulation presented in Section II allows for field excitations having higher order modes, the examples presented below are for the incident TEM mode only.

In the first case, we considered a uniformly loaded parallel-plate waveguide. This waveguide geometry makes a good case study since it can be simulated by a simple transmission line system. Fig. 3 shows good agreement obtained for the magnitude and phase as evaluated along an axial cut ($x = 0$), for a 0.3λ width waveguide. The lossy filling material had a relative permittivity of $\epsilon_r = (4.0 - j1.0)$. The terminal boundary Γ_B was placed, as shown in the inset to Fig. 1, at 0.1λ from the dielectric interface.

In the second geometry, we considered a 0.4λ waveguide having a circular dielectric cylinder with a radius of 0.14λ and $\epsilon_r = 4$ (see Fig. 4). Fig. 5 shows the contour plot for the normalized total H field superimposed on the waveguide geometry. The field lines can be observed to have a higher concentration inside the dielectric material.

As a third example, we considered an iris-loaded waveguide. From the perspective of the finite element modeling, it is important to assume here that the iris has a finite thickness. This is necessary to account for the differences in the surface currents flowing on each side of the iris. The assumed iris thickness was 0.01λ, and the finite element results are compared with those for the solution generated using the Wiener–Hopf technique [1]. Fig. 6 shows numerical results for the magnitude of the normalized H-field distribution along vertical cuts on both sides of the metallic iris, and their comparison with the Weiner–Hopf solution [1] for an infinitely thin iris. The good agreement shown in this figure was achieved even when the outer boundaries were placed as close as 0.2λ from the iris. This clearly demonstrates that the surface integral equation method can achieve numerical efficiency by reducing the size of the interior region and, hence, the number of finite element nodes.

IV. Conclusions

In this work, the surface integral equation has been used as a boundary condition for the finite element solution of the multiport waveguide discontinuity problem. The major advantage offered by the use of the surface integral equation approach is that it allows for placing the mesh-terminating outer boundaries of the finite element region as close to the junction discontinuity as possible, thus minimizing the size of the finite element matrix. This advantage is achieved despite the fact that the evanescent modes have significant amplitudes in the region close to the discontinuity. The accuracy of the surface integral equation formulation and its simplicity make it an efficient and versatile tool in the analysis of waveguide discontinuity problems.

References

[1] S. W. Lee, W. R. Jones, and J. J. Campbell, "Convergence of numerical solutions of iris-type discontinuity problems," *IEEE Trans. Microwave Theory Tech.*, vol. MTT-19, pp. 528–536, June 1971.

[2] R. Mittra and S. W. Lee, *Analytical Techniques in the Theory of Guided Waves*. New York, NY: MacMillan, 1971.

[3] P. P. Silvester and R. L. Ferrari, *Finite Elements for Electrical Engineers*, 2nd ed. Cambridge, England: Cambridge University Press, 1989.

[4] V. Kanellopoulos and J. P. Webb, "A complete E-plane analysis of waveguide junctions using the finite element method," *IEEE Trans. Microwave Theory Tech.*, vol. 38, pp. 290–295, Mar. 1990.

[5] B. H. McDonald and A. Wexler, "Finite element solution of unbounded field problems," *IEEE Trans. Microwave Theory Tech.*, vol. MTT-20, pp. 841–847, Dec. 1972.

[6] J. Jin and V. Liepa, "Application of hybrid finite element method to electromagnetic scattering from coated cylinders," *IEEE Trans. Antennas Propagat.*, vol. 36, pp. 50–54, Jan. 1988.

[7] O. M. Ramahi, "Boundary conditions for the solution of open-region electromagnetic scattering problems," Ph.D. dissertation, University of Illinois, Urbana, 1990.

[8] S. Kagami and I. Fukai, "Application of the boundary-element method to electromagnetic field problems." *IEEE Trans. Microwave Theory Tech.*, vol. MTT-32, pp. 455–461, Apr. 1984.

[9] M. Koshiba and M. Suzuki, "Application of the boundary-element method to waveguide discontinuities," *IEEE Trans. Microwave Theory Tech.*, vol. MTT-34, pp. 301–307, Feb. 1984.

[10] G. Strang and G. Fix, *An Analysis of the Finite Element Method*. Englewood Cliffs, NJ: Prentice-Hall, 1973.

[11] J. N. Reddy, *An Introduction to the Finite-Element Method*. New York, NY: McGraw-Hill, 1984.

[12] J. Stratton, *Electromagnetic Theory*. New York, NY: McGraw-Hill, 1941.

On the Use of Shanks's Transform to Accelerate the Summation of Slowly Converging Series

Surendra Singh and Ritu Singh

***Abstract*—It is shown that the application of Shanks' transform results in accelerating the convergence of slowly converging series. The transform is applied to a periodic Green's function involving a single summation. The convergence properties of this series are reported for the "on-plane" case, in which the series converges extremely slowly. Numerical results indicate that by employing Shanks's transform the computation time can be reduced by as much as a factor of 200.**

Manuscript received July 5, 1990; revised October 8, 1990.

The authors are with the Department of Electrical Engineering, University of Tulsa, Tulsa, OK 74104.

IEEE Log Number 9041945.

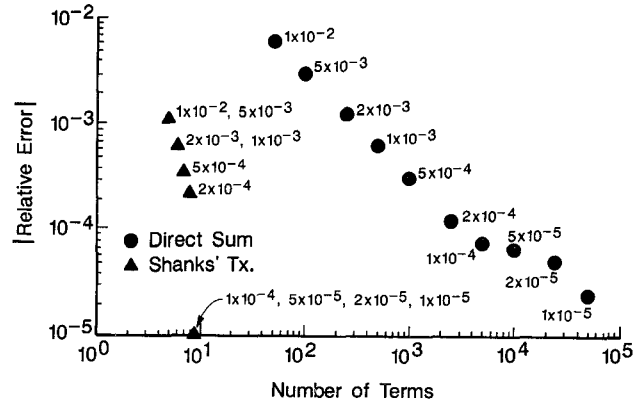

Fig. 1. Relative error magnitude versus number of terms for the series in (1) for $x = \pi/2$.

I. Introduction

In the analysis of periodic structures, one usually encounters a Green's function which converges very slowly. As repeated evaluations of the Green's function series are needed in determining the radiation or scattering from a periodic array using the method of moments with subsectionally defined basis functions, the slow convergence of the series would result in a considerable amount of computation time. In order to reduce this time, we look for ways to accelerate the convergence of the Green's function series. A method for improving the convergence of a doubly infinite periodic Green's function series has previously been suggested [1]–[3]. It has been successfully applied by a number of investigators to singly and doubly periodic Green's function series [4]–[8]. This paper reports the use of Shanks's transform in accelerating the convergence of a periodic Green's function involving a single infinite summation. Although the use of Shanks's transform in conjunction with Kummer's and Poisson's transformations has been shown in [3] to improve the convergence of a doubly periodic Green's function, it is reported here that a simple application of this transform alone to very slowly converging series enhances their convergence tremendously. Another advantage of using the transform is that no analytical work need be done to the series. This is an attractive feature, as the transform can be applied to a wide variety of series.

II. Illustrative Example of Shanks's Transform

If a sequence of partial sums of a series behaves as a "mathematical transient" as defined by Shanks in [9], then it is possible to extract the base of this "transient" by an application of Shanks's transform [9]. The transform is applied successively to the partial sums of the series until a predefined convergence criterion is satisfied. An algorithm to compute different orders of Shanks's transform is given in [10]. It is interesting to note that although the partial sums show no indication of converging to the sum of the series, the application of Shanks's transform is able to extract the sum from these partial sums. This is illustrated by taking the following series:

$$S = \sum_{n=1}^{+\infty} \frac{\sin(2n-1)x}{4\pi(2n-1)}. \tag{1}$$

0018-9480/91/0300-0608$01.00 ©1991 IEEE